Crack growth rate under variable T-stress

V.N. Shlyannikov and A.P. Zakharov

Research Center for Power Engineering Problems of the Russian Academy of Sciences
E-mail: shlyannikov@mail.ru

ABSTRACT. *This numerical and experimental study is directed to understanding the crack propagation under mixed mode biaxial loading. Subjects for studies are cruciform specimen under biaxial loading, central notched specimen and compact tension-shear specimen. The different degrees of mode mixity from pure mode I to pure mode II are given by the combinations of the far-field stress level, load biaxiality and inclined crack angle. This work is centered on the role of the T-stress during cyclic mixed mode fatigue crack growth. For the experimental crack paths in tested specimens mixed mode constraint parameters were calculated by finite element analysis. As result mixed mode fatigue fracture diagrams as a function the T-stress are obtained. The variation patterns of the crack growth rate with initial angle of crack inclination in specimens various configurations are given quantitatively. It is shown that there is a greater variation of mixed mode crack growth rate depending on current value of the T-stress along the curvilinear crack trajectories.*

INTRODUCTION

Recently several two parameter models to elastic-plastic fracture mechanics were introduced to explain some of the restriction inherent in the one parameter approach based on the *J*-integral and account for observed size and loading conditions effects on fracture toughness. It was shown that much of the dependence of fracture toughness on specimen geometry could be explained by two parameter fracture theories based on elastic and elastic-plastic constraint factors T, Q or A_2 [1-4]. Under small and moderate-scale yielding the T and Q approaches are essentially equivalent and A_2-approach is limited only pure mode I fracture. The elastic T-stress, the second term of the asymptotic series for the stress field in a linear elastic material, has also been used to characterize constraint in mode I and mixed mode loading. It is often postulated for linear elastic materials that the effect of dimensionless crack length on T-stress on mode I brittle fracture can be ignored. However, it is shown [5] that the T-stress is no longer constant along the curvilinear crack paths for fracture specimens various geometries and depends on the both initial size and angle of crack under mixed mode loading.

In this paper, the T-stress originally proposed to two parametrical describe fracture toughness for pure mode I under *monotonic/static* loading, is employed to study the crack growth rate under *cyclic* mixed mode fracture. Earlier numerical and experimental results are used to corroborate the findings.

T-STRESS DETERMINATION

Subjects for studies are cruciform specimen under biaxial loading, central notched specimen and compact tension-shear specimen (Fig.1). Different degrees of mode mixity from pure mode I to pure mode II are given by combinations of the far-field stress level σ, biaxial stress ratio η and inclined crack angle α.

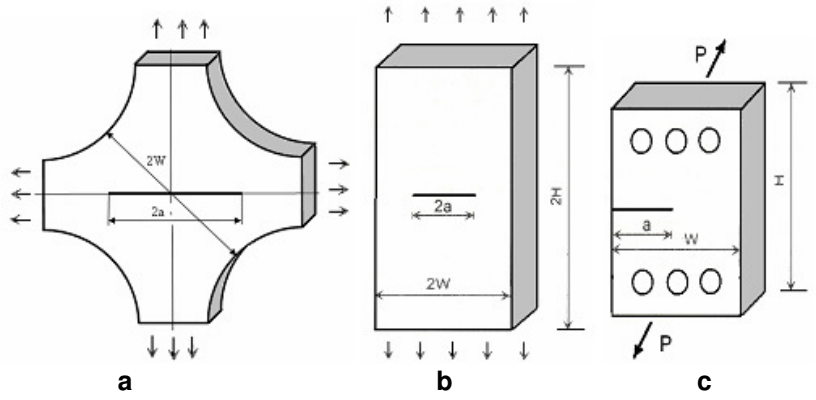

Figure 1. (a) Cruciform specimen (CS), (b) central notched specimen (CNS) and (c) compact tension-shear specimen (CTS).

All investigated configurations contain an internal crack of length *2a* for CS and CNS or *a* for CTS, which is angled to the edges of the specimens. The cruciform specimen is subjected by uniform stress of magnitude σ and 0.5σ along the remote edges parallel to the *Y* and *X* axes, respectively. The initial crack makes on angle α with the loading direction. For the biaxially loaded CS $\alpha = 0^\circ$ or $\alpha = 90^\circ$ correspond to pure mode I, while at $0^\circ < \alpha < 90^\circ$ can be achieved mixed mode fracture. In the CTS $\alpha = 90^\circ$ correspond to pure mode I and pure mode II can be achieved when $\alpha = 0^\circ$. Finally, for the CNS $\alpha = 90^\circ$ correspond to pure mode I.

The principal moment of our study is the use of elastic *T*-stress as some additional governing parameter of the crack growth rate. Author [5] considered the *T*-stress determination along experimental curvilinear crack paths for the most popular mixed mode fracture specimens. This study explores direct use of FEM analysis for calculating *T*-stress on the base of crack flank nodal displacements [6]. Using this technique, the *T*-stress distributions in various specimen geometries was determined from numerical calculations. On this basis the solutions for mode I and mode II stress intensity factors K_1 and K_2 for each specimen geometry have been obtained [5].

The normalized *T*-stress distributions of various fracture specimen geometries under mixed mode loading conditions are determined from finite element calculations. Figure 2 is a plot of the *T*-stress ahead of the crack-tip ($\theta=0^\circ$) as a function of an initial crack angle α and relative crack length *a/w* for different specimen geometries. Note that the deviation of current value of *T* from the corresponding original value for a/w=0.1 (or a/w=0.5 for CTS) increases with increasing relative crack length at fixed crack angle position.

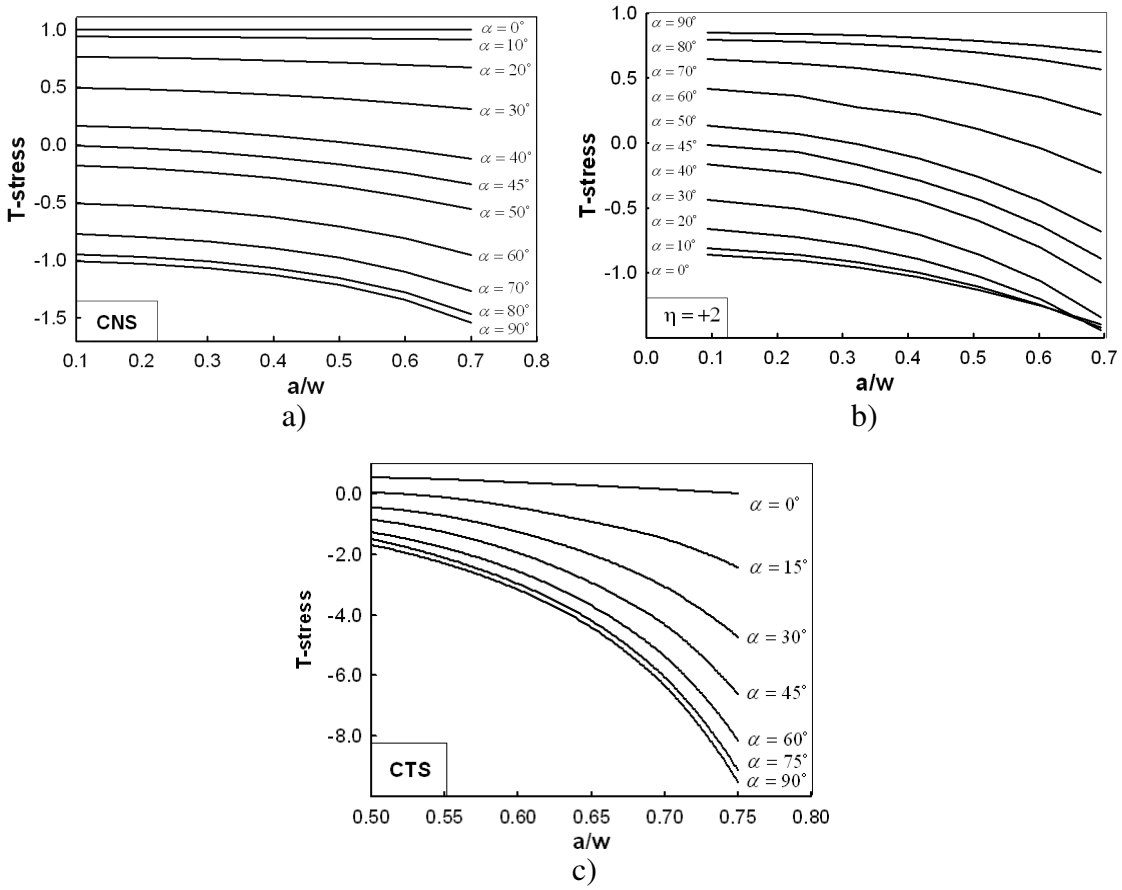

Figure 2. Mixed mode *T*-stress distributions of (a) CNS, (b) CS and (c) CTS geometries.

By fitting the numerical calculations, the constraint parameter *T*-stress and the mixed mode stress intensity factors as the function of varied crack length and crack angle for particular geometry considered were represented in the form of the approximation equations. The length, angle and geometry correction factors for all specimen configurations analysed in this study was obtained by curve fitting. The equations for these factors in terms of geometrical parameters are as follows:

$$\overline{T} = A_1\left(\frac{a}{w}\right)^2 + A_2\left(\frac{a}{w}\right) + A_3 \qquad \text{for CS and CNS} \qquad (2)$$

$$\overline{T} = A_1\left(\frac{a}{w}\right)^3 + A_2\left(\frac{a}{w}\right)^2 + A_3\left(\frac{a}{w}\right) + A_4 \qquad \text{for CTS} \qquad (3)$$

where a is crack length and w is specimen width. Full expressions for all coefficients A_i as a function of crack inclination angle α for various fracture specimens geometries are the following:

Cruciform specimen with remote biaxial ratio $\eta = 0.5$

$$A1(\alpha) := -2.662728741\cdot10^{-7}\cdot\alpha^4 + 4.118165741\cdot10^{-5}\cdot\alpha^3 - 1.142843121\cdot10^{-3}\cdot\alpha^2 - 2.804993231\cdot10^{-2}\cdot\alpha - 1.198771$$
$$A2(\alpha) := -1.157027651\cdot10^{-8}\cdot\alpha^4 + 4.22696721\cdot10^{-6}\cdot\alpha^3 - 4.801376241\cdot10^{-4}\cdot\alpha^2 + 1.772144181\cdot10^{-2}\cdot\alpha + 6.460320331\cdot10^{-2}$$
$$A3(\alpha) := -5.322598771\cdot10^{-6}\cdot\alpha^3 + 7.243427751\cdot10^{-4}\cdot\alpha^2 - 3.234349811\cdot10^{-3}\alpha - 8.548286661\cdot10^{-1}$$

Central notched specimen

$$A1(\alpha) := 4.245104911\cdot10^{-6}\cdot\alpha^3 - 6.056922551\cdot10^{-4}\cdot\alpha^2 + 1.939424141\cdot10^{-3}\cdot\alpha - 3.248315321\cdot10^{-3}$$
$$A2(\alpha) := -9.552059051\cdot10^{-7}\cdot\alpha^3 + 2.188184471\cdot10^{-4}\cdot\alpha^2 - 6.819771311\cdot10^{-3}\cdot\alpha + 2.010807371\cdot10^{-2}$$
$$A3(\alpha) := 6.131643361\cdot10^{-6}\cdot\alpha^3 - 8.369487971\cdot10^{-4}\cdot\alpha^2 + 2.96425541\cdot10^{-3}\cdot\alpha + 9.958028931\cdot10^{-1}$$

Compact tension-shear specimen

$$A1(\alpha) := \left[\left(\alpha^3\right)\cdot\left(9.636604461\cdot10^{-4}\right) - \left(\alpha^2\right)\cdot\left(1.064862331\cdot10^{-1}\right) - (\alpha)\cdot(3.1988822 \right. \left. + 4.8782459\right]$$
$$A2(\alpha) := \left[-\left(\alpha^3\right)\cdot\left(1.760725331\cdot10^{-3}\right) + \left(\alpha^2\right)\cdot\left(2.057783401\cdot10^{-1}\right) + (\alpha)\cdot(3.7451356 \right. \left. 5\right] - 1.194250441$$
$$A3(\alpha) := \left(\alpha^3\right)\cdot\left(1.071745661\cdot10^{-3}\right) - \left(\alpha^2\right)\cdot\left(1.297132931\cdot10^{-1}\right) - (\alpha)\cdot(1.4262827 \left. 8 + 7.051961\right.$$
$$A4(\alpha) := \left[-\left(\alpha^3\right)\cdot\left(2.150554801\cdot10^{-4}\right) + \left(\alpha^2\right)\cdot\left(2.672064631\cdot10^{-2}\right) + (\alpha)\cdot\left(1.435047621\cdot10^{-1}\right)\right] - 6.156324381\cdot10^{-1}$$

It should be noted that for in-plane mixed mode fracture conditions takes place two form of the crack tip displacement characterized by the corresponding stress intensity factors K_1 and K_2. This fact predestines the need to use in order of mixed mode fatigue experimental data interpretation the effective stress intensity factor K_{eff} which is function both K_1 and K_2. In our method of mixed mode fatigue experimental result interpretation we have used effective stress intensity factor in the form of the strain energy density factor S [7]

$$S = b_{11}K_1^2 + 2b_{12}K_1K_{11} + b_{22}K_{11}^2 \qquad \left.\begin{aligned} b_{11} &= \frac{1}{16G}(\kappa - \cos\theta)(1+\cos\theta) \\ b_{12} &= \frac{2}{16G}(\cos\theta - \kappa + 1)\sin\theta \\ b_{22} &= \frac{1}{16G}[(\kappa+1)(1-\cos\theta) + \\ &+ (3\cos\theta - 1)(1+\cos\theta)] \end{aligned}\right\} \qquad (4)$$

In the method suggested by authors [8] for the experimental data interpretation, based on the concept of a straightline crack, crack growth is connected to a variation in the inclined crack angle. This fact predestines the need to transfer from one function

$Y_1\big|_{\beta_i=const}$ (or $Y_2\big|_{\beta_i=const}$) to another one. Therefore when calculating the stress intensity factors K_1 and K_2 double interpolation was carried out the Y_1 and Y_2 functions by both the crack length and its inclined angle using Lagrange polynomial.

The experimental study of fatigue crack growth rate in the aluminum alloy is performed on biaxially loaded cruciform specimen. All specimens for biaxial loading contained inclined through thickness central cracks. Mixed mode I/II fatigue crack growth rate experiments on the high-strength steel and the titanium alloy used the compact tension shear and the center notched specimens consequently. The main mechanical properties for tested materials are listed in Table 1.

CS tests have been carried out under biaxial tension with nominal stress ratio η=0.5 on the special test-machine with frequency 5 Hz at stress ratio 0.1. CNS and CTS tests have been performed on the MTS Landmark test-machine with frequency 10 Hz at stress ratio 0.1.

Table 1. Mechanical properties

Material	Yield stress R_e (MPa)	Ultimate stress R_m (MPa)	Reduction of area (%)	Strain hardening exponent
Aluminum alloy	160	384	25	4.29
Steel	1039	2064	45	6.43
Titanium alloy	508	534	11	9.29

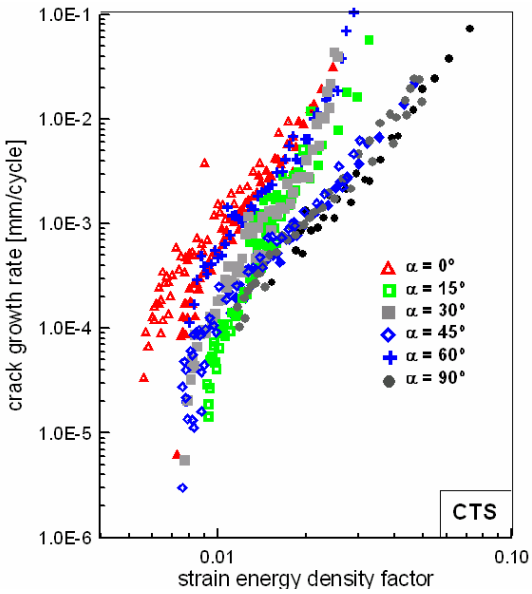

Figure 3. Mixed-modes fatigue fracture diagram of CTS geometry.

The typical experimental fatigue fracture diagrams in coordinates of the crack growth rate versus the strain energy density factor for all investigated titanium CTS specimens for full range of mixed mode loading are shown in Fig.3. Mode I crack growth corresponds to $\alpha = 90^{\circ}$ and $\alpha = 0^{\circ}$ is pure mode II while $\alpha < 90^{\circ}$ represents mixed mode crack growth. Figure 3 shows that mixed mode-loading causes a significant increase in crack growth rate with respect to pure mode I for all tested CTS specimens. Moreover, the crack growth rate monotonically increases when mode mixity changed from pure mode I to pure mode II.

By substituting the experimental values of the crack length increment and the crack angle deviation in the approximation equation (2-3) describing the *T*-stress behavior, the current values of the constraint parameter were obtained for each specimen. Graphs showing these experimental results are presented in Fig. 4.

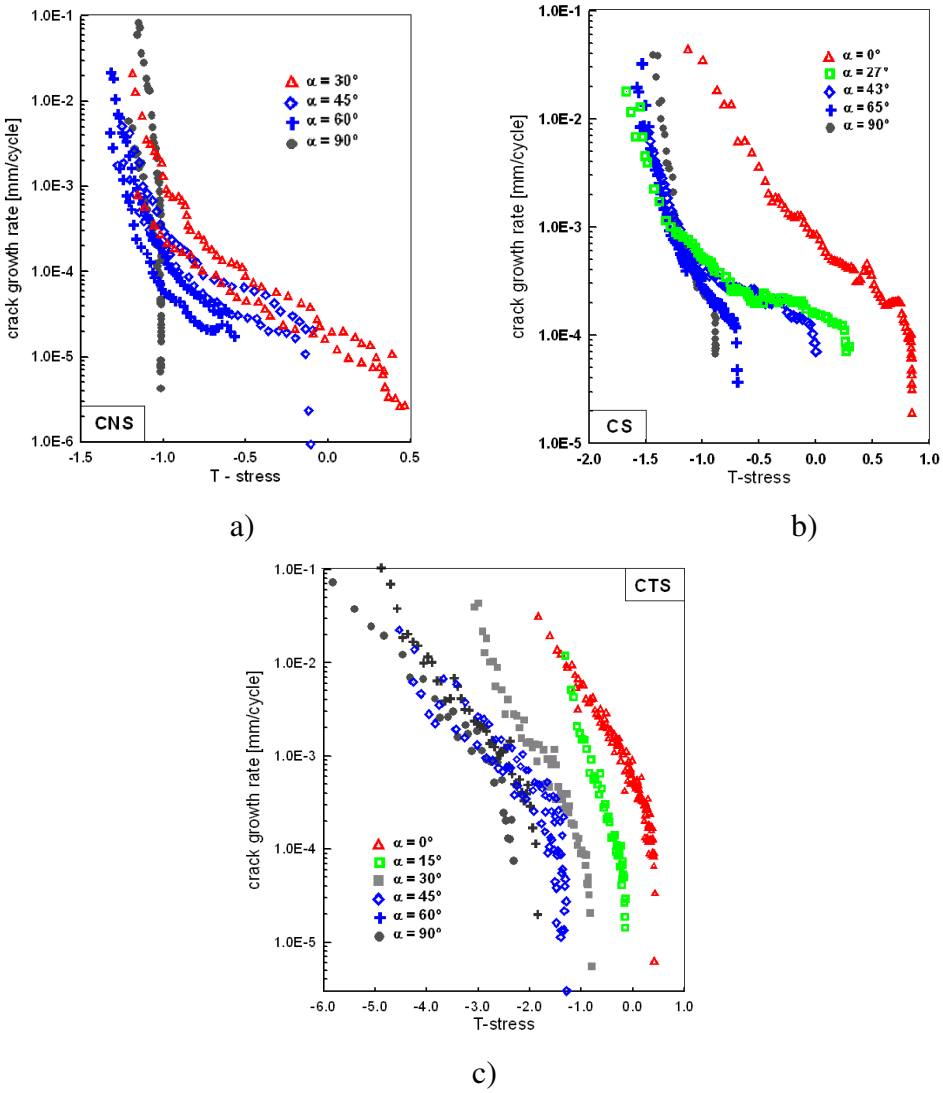

Figure 4. Crack growth rate versus *T*-stress of (a) CNS, (b) CS and (c) CTS geometries.

Represented experimental results show that the general for all tested specimens and materials of different properties is a trend of increasing crack growth rate while decreasing the constraint effects characterized by the *T*-stress. As follows from the data within each individual fatigue fracture diagram more constrained conditions in the specimens studied geometries cause the lower rate of crack growth. It is shown in Fig.4 that there is a greater variation of mixed mode crack growth rate depending on current value of the T-stress along the curvilinear crack trajectories. Positive values of the *T*-stress correspond to lower values of fatigue crack growth rate. Influence of mixed mode loading on the crack growth rate in the interpretation through the constraint parameter is also monotonic. From a comparison of the diagrams of fatigue fracture as a function of the equivalent stress intensity factor and the *T*-stress follows that the crack growth rate should be more sensitive to change of constraint factor. Therefore varied values of *T*-stress can be an additional parameter characterizing the crack growth rate under mixed modes of loading.

CONCLUSION

This work is centered on the role of the T-stress during cyclic mixed mode fatigue crack growth. In the present study it is stated that the *T*-stress is not constant and demonstrated how it changes depending on crack length and crack angle combinations in fracture specimens various configurations. It is shown that there is a greater variation of mixed mode crack growth rate depending on current value of the T-stress along the curvilinear crack trajectories.

ACKNOWLEDGMENT

The authors gratefully acknowledges the financial support of the Russian Foundation for Basic Research under the Project 12-08-97085p.

REFERENCES

1. Betegon, C. and Hancock, J.W. (1991) *J. Appl. Mech.* **58**, 104-110.
2. O'Dowd N.P. and Shih, C.F. (1991) *J. Mech. Phys. Solids* **39**, 989-1015.
3. Yang, S., Chao Y.J. and Sutton, M.A. (1993) *Engng. Fract. Mech.* **45**, 1-20.
4. Nikishkov G.P. (1995) *Engng. Fract. Mech.* **50**, 65-83.
5. Shlyannikov, V.N. (2012) *Proc. Fourth Int. Conf. CP 2012*, Gaeta, Italy, 643-650.
6. Ayatollahi, M.R., Pavier, M.J., Smith, D.J. (1998) *Int. J. Fract.* **91**, 283-298.
7. Sih, G.C. (1974) *Int. J. Fracture* **10**, 305-321.
8. Shlyannikov, V.N. and Braude, N.Z. (1992) *Fatigue Fract. Engng. Mater. Struct.* **15**, 825-844.